machine learning & knowledge extraction

MDPI

Article

Balancing Results from AI-Based Geostatistics versus Fuzzy Inference by Game Theory Bargaining to Improve a Groundwater Monitoring Network

Masoumeh Hashemi [1,*], Richard C. Peralta [2,*] and Matt Yost [1]

[1] Plant, Soil & Climate Department, Utah State University, Logan, UT 84322, USA; matt.yost@usu.edu
[2] Civil and Environmental Engineering Department, Utah State University, Logan, UT 843322, USA
* Correspondence: masoumeh.hashemi@usu.edu (M.H.); richard.peralta@usu.edu (R.C.P.); Tel.: +1-435-470-7593 (M.H.); +1-435-881-4947 (R.C.P.)

Abstract: An artificial intelligence-based geostatistical optimization algorithm was developed to upgrade a test Iranian aquifer's existing groundwater monitoring network. For that aquifer, a preliminary study revealed that a Multi-Layer Perceptron Artificial Neural Network (MLP-ANN) more accurately determined temporally average water table elevations than geostatistical kriging, spline, and inverse distance weighting. Because kriging is usually used in that area for water table estimation, the developed algorithm used MLP-ANN to guide kriging, and Genetic Algorithm (GA) to determine locations for new monitoring well location(s). For possible annual fiscal budgets allowing 1–12 new wells, 12 sets of optimal new well locations are reported. Each set has the locations of new wells that would minimize the squared difference between the time-averaged heads developed by kriging versus MLP-ANN. Also, to simultaneously consider local expertise, the algorithm used fuzzy inference to quantify an expert's satisfaction with the number of new wells. Then, the algorithm used symmetric bargaining (Nash, Kalai–Smorodinsky, and area monotonic) to present an upgradation strategy that balanced professional judgment and heuristic optimization. In essence, the algorithm demonstrates the systematic application of relatively new computational practices to a common situation worldwide.

Keywords: bargaining theory; fuzzy inference system; groundwater monitoring; geostatistics; artificial neural network; optimization

Citation: Hashemi, M.; Peralta, R.C.; Yost, M. Balancing Results from AI-Based Geostatistics versus Fuzzy Inference by Game Theory Bargaining to Improve a Groundwater Monitoring Network. *Mach. Learn. Knowl. Extr.* **2024**, *6*, 1871–1893. https://doi.org/10.3390/make6030092

Academic Editors: Amir Masoud Rahmani, Danial Javaheri and Hassan Chizari

Received: 1 July 2024
Revised: 6 August 2024
Accepted: 7 August 2024
Published: 9 August 2024

1. Introduction

Groundwater level maps are crucial raster data that relate aquifer hydraulic conductivity, recharge zones, flow directions, velocity, and management strategies. They also assist in operations, i.e., their conservation policies. A groundwater level monitoring network is essential for managing groundwater [1,2]. However, installing observation wells throughout an aquifer is impractical [3,4]. Consequently, many researchers have focused on improving head estimation for unmonitored sites [5,6]. The accuracy of estimating groundwater heads at unmeasured locations depends on the number and location of monitoring wells and varies spatially with the surface fitting method [6,7].

The process of determining unknown values between known values is called interpolation. Surface fitting methods are used to interpolate the value at unknown points. These methods can be classified as follows: I: deterministic (e.g., spline, inverse distance weighting (IDW), etc.); II: geostatistical (e.g., kriging, universal kriging, etc.) [8]; and III: machine learning [6]. Of the geostatistical methods used to develop water table maps from observed water levels by surface fitting [9], kriging is the most common [10,11]. Machine learning has been applied to estimate or predict groundwater levels [6,12] and to predict other water-related variables [13].

The accuracy of interpolations depends on the number and spatial distribution of monitoring locations [11,14]. To improve the accuracy of estimation at unmonitored points, the importance of implementing observation well monitoring programs has attracted the attention of many authors [15,16]. Model fitting and interpolation methodologies can differ for site-specific conditions. Utilized optimization objective functions include reducing the long-term monitoring cost [5], maximizing spatial accuracy and minimizing temporal redundancy in head observations [16,17], minimizing standard deviations in predicted head error by adding new wells and eliminating wells [18,19], improving the reliability of groundwater simulation model predictions [20,21], and optimizing the number of monitoring stations and sampling intervals [22,23]. As far as the design of monitoring networks is concerned, there is no single right or wrong method, and often, judgment should be based on the expertise of the personnel designing the network rather than on statistical or modeling results [24,25].

Ideally, the design should employ (i) qualitative and quantitative hydrogeological information and statistical approach(es) that might include statistical analysis, interpolation methods, contaminant transport simulations, and/or numerical groundwater flow [24,26] and (ii) local experts' experience [24]. To represent an expert's opinion, a Fuzzy Inference System (FIS) uses fuzzy logic and set theory to convert fuzzy qualitative input values into crisp numeric values. Two types of widely used FIS [27] are Mamdani [28] and Sugeno [29]. To date, FIS has been used in groundwater management for estimating groundwater levels [30–32] but has not been utilized in improving a groundwater monitoring network.

The primary objective of this research was to integrate expert insights into a framework aimed at pinpointing optimal locations for new observation wells, thereby enhancing the precision of kriged groundwater level maps. Initially, it discerned the most precise surface fitting method for delineating groundwater levels within the study area, namely, the Qazvin plain in Iran. Subsequently, the study proposed strategies for augmenting groundwater level monitoring networks via heuristic optimization, which involved identifying prime sites for new wells and incorporating expert judgments through fuzzy logic. This study introduced an innovative methodology that orchestrated multiple processes concurrently and sequentially to systematically juxtapose and harmonize numerical optimization outcomes with expert-derived site-specific knowledge. Notably, this methodology introduced the inaugural FIS designed specifically to encapsulate expert judgment in enhancing groundwater level monitoring networks.

2. Materials and Methods

2.1. Study Area

Due to excessive groundwater extraction, over one-third of Iran's plains are now designated as prohibited zones for new well drilling [33,34]. In the 3919 km^2 Qazvin Aquifer, groundwater levels have steadily decreased over the years, leading to limitations on groundwater extraction in areas classified as prohibited plains where new extraction well drilling is prohibited [11,35]. This region has an annual mean temperature of 13 °C, an annual precipitation of about 320 mm, and a cold-dry climate (Figure 1). Groundwater levels, as monitored by 168 observation wells, exhibit an average monthly range between 1129.5 m and 1408.3 m.

Considering the aquifer's important role as a primary source of irrigation water, water managers are motivated to refine their estimations of groundwater volumes [11]. With a focus on aiding the Qazvin Regional Water Company (QRWC), this study aims to elucidate the most efficacious methodology for increasing the accuracy of widely utilized groundwater level data through the integration of additional groundwater level observation wells. Acknowledging the inherent temporal variability of groundwater, including fluctuations within each year, the study adopts the mean head derived from a comprehensive dataset encompassing 72 consecutive months of monthly measurements as the target water level at each pre-existing observation site.

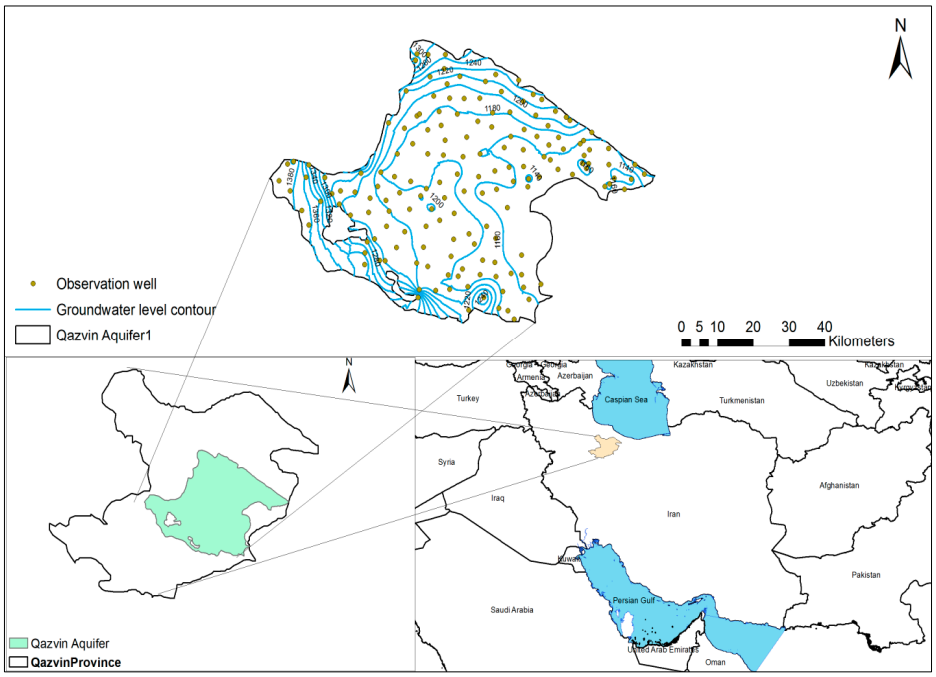

Figure 1. Groundwater level contours and observation wells in Qazvin Aquifer, Qazvin Province, Iran.

2.2. Comparison of Groundwater Surface Mapping Methods for the Study Area

In the study area, water managers have traditionally relied on kriging to generate water table maps [11]. Kriging head values are derived from an existing monitoring well network. There is commonly overestimation and underestimation of values for locations without observed data [36]. In our study, comparative analyses are performed between kriging [37], inverse distance weighting (IDW) [38,39], spline [40,41], and Multi-Layer Perceptron Artificial Neural Network (MLP-ANN) [42].

To conduct these analyses, a Kriging MATLAB toolbox [43] was added to the MATLAB toolboxes, and the neural network toolboxes were utilized for MLP-ANN. For spline and IDW methods, we used Arc GIS. Observed head values were divided into two groups: training and testing. The accuracy of each method was evaluated to estimate the heads of the testing sets.

2.2.1. Kriging

Kriging is the most used technique for mapping geologic and hydrological surfaces [44,45]. To estimate a value at a specified location, kriging considers both the distance between known observation locations and the difference in their observed values. To estimate a value at a location without direct measurement, kriging employs observed data and weights as specified within Equation (1).

$$H^*(x) = \sum_{i=1}^{N_m} \frac{1}{2N(h)} \sum_{i=1}^{N(h)} (H(X_i) - H(X_i + h))\, H(x_i) \quad (1)$$

where $H^*(x)$ is the groundwater level estimated by kriging, N_m is the number of observation wells, $H(X_i)$ is the groundwater level measured at the ith location, and N(h) is the total number of pairs of employed observation locations that are separated by a distance h. The weight is calculated by applying equations that use a site-specific semivariogram [37,39].

To adequately describe site-specific regional geologic trends, it is crucial to utilize an appropriate form of semivariogram. Within the study area, statistical indicators are employed to assess and contrast five types of theoretical variograms: spherical, exponential, Gaussian, linear, and power function. Within the outlined methodology, the semivariogram offering the most accurate estimation of head size is identified. For each semivariogram, the

evaluation process involves dividing observed field data into 70% training and 30% testing sets, determining kriging that optimizes the agreement between observed and estimated (kriged) heads, applying these weights to estimate heads at testing dataset locations, and calculating statistical metrics.

2.2.2. Inverse Distance Weighting (IDW)

In IDW interpolation, a set of sample points is linearly weighted to determine a value for an unmeasured location. These weights are determined by the inverse distance between the measured and predicted locations, meaning that points closer to the predicted location exert more influence on its value compared to those farther away. The computation of the value for unmeasured points is performed using the following equation:

$$H^*(x_0) = \sum_{i=1}^{N_m} \frac{\frac{1}{d_i}}{\sum_{i=1}^{n}\left(\frac{1}{d_i}\right)} H(x_i) \quad (2)$$

where d_i is the distance from the ith measured point (x_i) to the predicted point (x_0). The same evaluation process is applied to assess the performance of this method.

2.2.3. Spline

The spline interpolation method utilizes a mathematical function to minimize overall surface curvature, resulting in a smooth surface that precisely intersects the measured points. This function can be expressed as follows:

$$S(x, y) = T(x, y) + \sum_{i=1}^{N_m} \lambda_i R(r_i) \quad (3)$$

where λ_i is the coefficient found by solving a system of linear equations, r_i is the distance between the predicted point and the ith point, S(x,y) is the new point of interpolation, and $T(x, y)$ and $R(r_i)$ are defined differently based on the selected option, which is the regularized option in this study. For additional details, consult references [40,41]. To statistically evaluate the performance of the interpolation method, testing data that were not used for training are employed.

2.2.4. Artificial Neural Network (ANN)

Artificial Neural Networks (ANNs) use simple information to help describe a complex system [1,46]. Among machine learning algorithms, artificial neural networks stand out for their capacity to discern intricate patterns from data [6,47]. While a range of machine learning algorithms exists for estimating groundwater levels [6,48], this study aims to construct a model that requires minimal input data that are both easy and inexpensive to collect. Thus, a feed-forward back-propagation neural network algorithm featuring a Multi-Layer Perceptron (MLP-ANN) architecture is developed for estimating the water table at a designated location (Figure 2). A previously reported MLP-ANN [6] employed latitude and longitude as inputs, and one hidden layer was not as accurate as kriging. The new MLP-ANN presented here additionally employed ground elevation as input and incorporated more than one hidden layer, as suggested in [6], to improve interpolation accuracy.

An MLP-ANN having hidden layers is a function, $f : \mathbb{R}^I \rightarrow \mathbb{R}^O$, where $\mathbb{R}$ is the set of real numbers, I is the size of the input vector, and O is the size of the output vector $F_O(x)$, such that the matrix notation is as follows:

$$O(I) = F_O(b_O + w_O(F_H(b_H + w_H(I)))) \quad (4)$$

where b_H and b_O are the bias matrices of the hidden layer and output layer, respectively; w_H and w_O are the weight matrices of the hidden layer and output layer, respectively; and F_H and F_O are transfer functions.

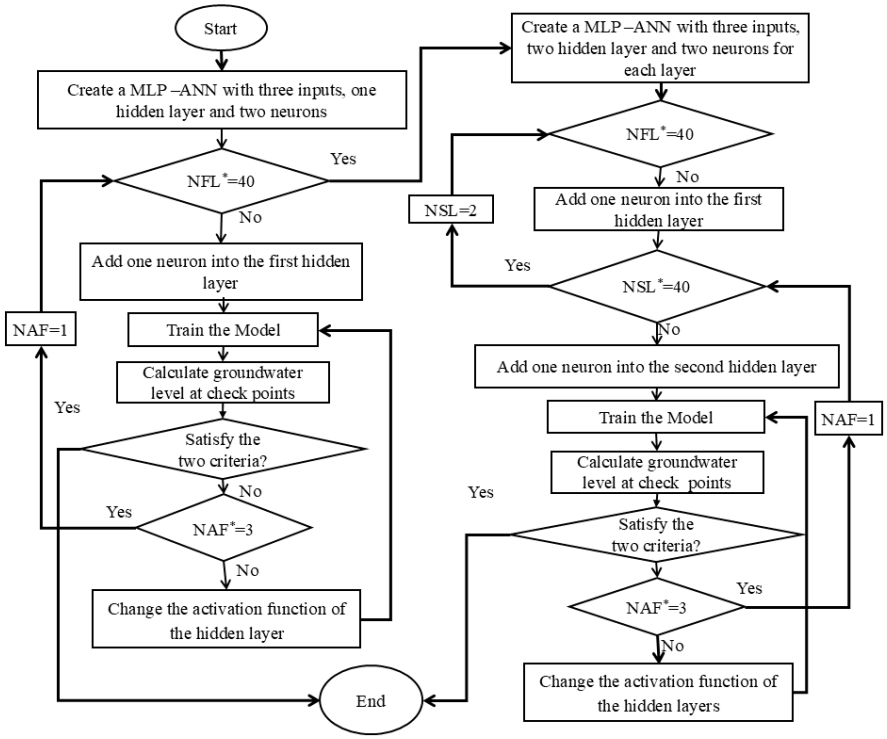

Figure 2. Conceptual architecture of employed hidden layer perceptron (NFL = number of neurons in the first layer; NSL = number of neurons in the second layer; NAF = number of activation functions).

The designed MLP-ANN calculated the groundwater level map using three inputs (longitude, latitude, and elevation) and used back-propagation to learn the network. The MPL-ANN is created using a neural network toolbox. To select an appropriate network, the data were randomly partitioned into two sets: 70% for training and 30% for testing. We selected the only MLP-ANN that satisfied two criteria: (i) a coefficient of determination higher than 0.9 and (ii) no estimated groundwater heads above the ground surface.

As shown in Figure 2, the first step started with a network that had one hidden layer and three neurons. The number of neurons was changed from 3 to 40. For each new number of neurons, three different activation functions—log-sigmoid, hyperbolic tangent sigmoid, and linear—were tested for the hidden layer. To evaluate each architecture, the same testing and training data were used. After that, the performance of each architecture was assessed based on the two criteria.

For the first criterion, the coefficient of determination (R^2) was calculated for the testing data. For the second criterion, 47,500 uniformly spaced check points that were 280 m apart (Figure 3) were provided. Groundwater levels at the check points were calculated and compared to the corresponding ground elevations. If no network met the two criteria, the number of neurons in the first layer could increase up to 40, and for each added neuron, the three activation functions could be evaluated. Following this step, one hidden layer could be added if the network did not still meet two criteria, so that the network was trained with two hidden layers. In this case, the first hidden layer had three neurons, and the second layer's neuron could change from 3 to 40. Furthermore, the activation function of hidden layers could be changed. Consequently, if it did not satisfy the criteria, one neuron could be added into the first hidden layer, making four neurons, and the second layer could change from 3 to 40 neurons to meet two criteria again. The cycle was continued until the created network satisfied both criteria.

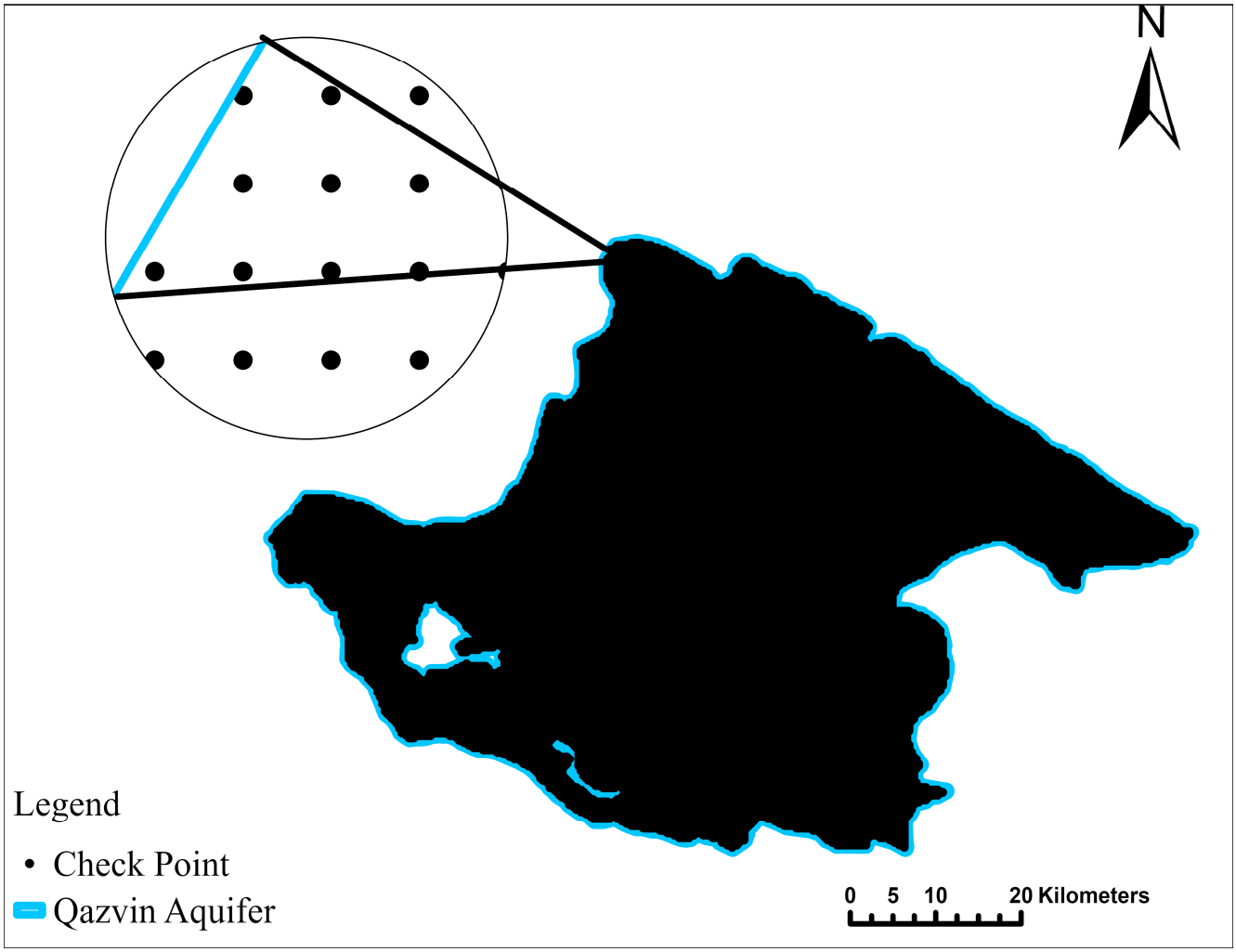

Figure 3. The check point locations (spaced 280 m apart).

2.2.5. Cross-Validation for Evaluation of Surface Fitting Methods

For each method, evaluation involves partitioning observed field head data into a training set and a testing set. Each method's training involves developing the set of weights or coefficients that cause the method's estimated heads to the best match observed training heads. Then, each trained method is used to estimate the heads of the testing dataset. The same testing and training sets have been used to evaluate the methods. The coefficient of determination (R^2), Root Mean Squared Error (RMSE), Mean Absolute Error (MAE), Root Mean Squared Logarithmic Error (RMSLE), and Relative Absolute Error (RAE) are used to evaluate how well each method estimates water levels at locations not used in training. Expressions of these parameters are shown in Equations (5)–(9):

$$R^2 = 1 - \frac{\sum_{i=1}^{N_{test}} \left(h_i^{obs} - h_i^{p}\right)^2}{\sum_{i=1}^{N_{test}} \left(h_i^{obs} - \overline{h}^{obs}\right)^2} \quad (5)$$

$$RMSE = \sqrt{\frac{\sum_{i=1}^{N_{test}} \left(h_i^{obs} - h_i^{p}\right)^2}{N_{test}}} \quad (6)$$

$$MAE = \frac{1}{N_{test}} \sum_{i=1}^{N_{test}} \left|h_i^{obs} - h_i^{p}\right| \quad (7)$$

$$\mathrm{RMSLE} = \sqrt{\frac{1}{\mathrm{N_{test}}}\sum_{\mathrm{i=1}}^{\mathrm{N_{test}}}\left(\log\left(\mathrm{h_i^{obs}}+1\right)-\log\left(\mathrm{h_i^{p}}+1\right)\right)^2} \quad (8)$$

$$\mathrm{RAE} = \frac{\sum_{\mathrm{i=1}}^{\mathrm{N_{test}}}\left|\mathrm{h_i^{p}}-\mathrm{h_i^{obs}}\right|}{\sum_{\mathrm{i=1}}^{\mathrm{N_{test}}}\left|\mathrm{h_i^{p}}-\overline{\mathrm{h}}^{\mathrm{obs}}\right|} \quad (9)$$

where N_{test} is the number of elements within the testing subset, h_i^{obs} is the observed groundwater level at the ith station, h_i^p is the predicted groundwater level at the ith station, and $\overline{h}^{obs}$ is the average of observed groundwater levels.

The testing process outlined above identifies the method that offers the closest matches between estimated groundwater heads and observed groundwater heads. Subsequently, the novel methodology described below is employed to determine the requisite number and locations of additional observation well(s) necessary to achieve the study's objectives.

2.3. Designed Methodology and Model

The procedural goal is to determine the number and locations of new observation wells to be added to an existing observation network. To maximize simultaneously both quantitative accuracy improvement and qualitative Satisfaction of the Expert, the presented procedure uses multiple tools simultaneously, iteratively, and sequentially to develop trade-off curves, and then applies game theory to select a compromise strategy. Figure 4 illustrates the flowchart of the proposed model.

Overall, the user is first requested to enter the Maximum Number of Added Wells (MNAWs) to be considered for addition to the monitoring network. The subsequent process is divided into two main phases:

- Phase 1: This phase is executed MNAW times to construct a Pareto optimum trade-off curve. It is further subdivided as follows:
    - Phase 1a: For each specified Number of Additional Wells (NOAWs) (ranging from 1 to MNAW), the model employs kriged groundwater level, the most accurate interpolation method, combined with a heuristic optimization algorithm. This phase aims to identify new well location(s) that will maximize the improvement in water level representation achieved through the kriging method.
    - Phase 1b: This phase utilizes an FIS to incorporate local expert opinions regarding the preferred number of a new well(s) and the unit cost of a new well.
    - Phase 1c: After executing phases 1a and 1b MNAW times, phase 1c constructs the Pareto optimum curve. This curve visualizes the trade-off between accuracy improvement from phase 1a vs. the expert opinion from phase 1b. It provides a comprehensive view of potential conflicts and compromises between numerical optimization and experiential input.
- Phase 2: In this phase, three game theory techniques are applied to the Pareto optimum curve to identify equilibrium strategies. By applying these game theory techniques, the model identifies the most balanced and effective strategies for well placement, considering both numerical accuracy and expert opinions. These strategies help ensure that the final decision on the number and location of new wells is both optimal and equitable.

Based on the outcomes of Phase 1 and Phase 2, the model user selects the number of new wells to be installed at the locations specified by the model. The detailed procedures and methodologies employed in each phase are explained in the following sections.

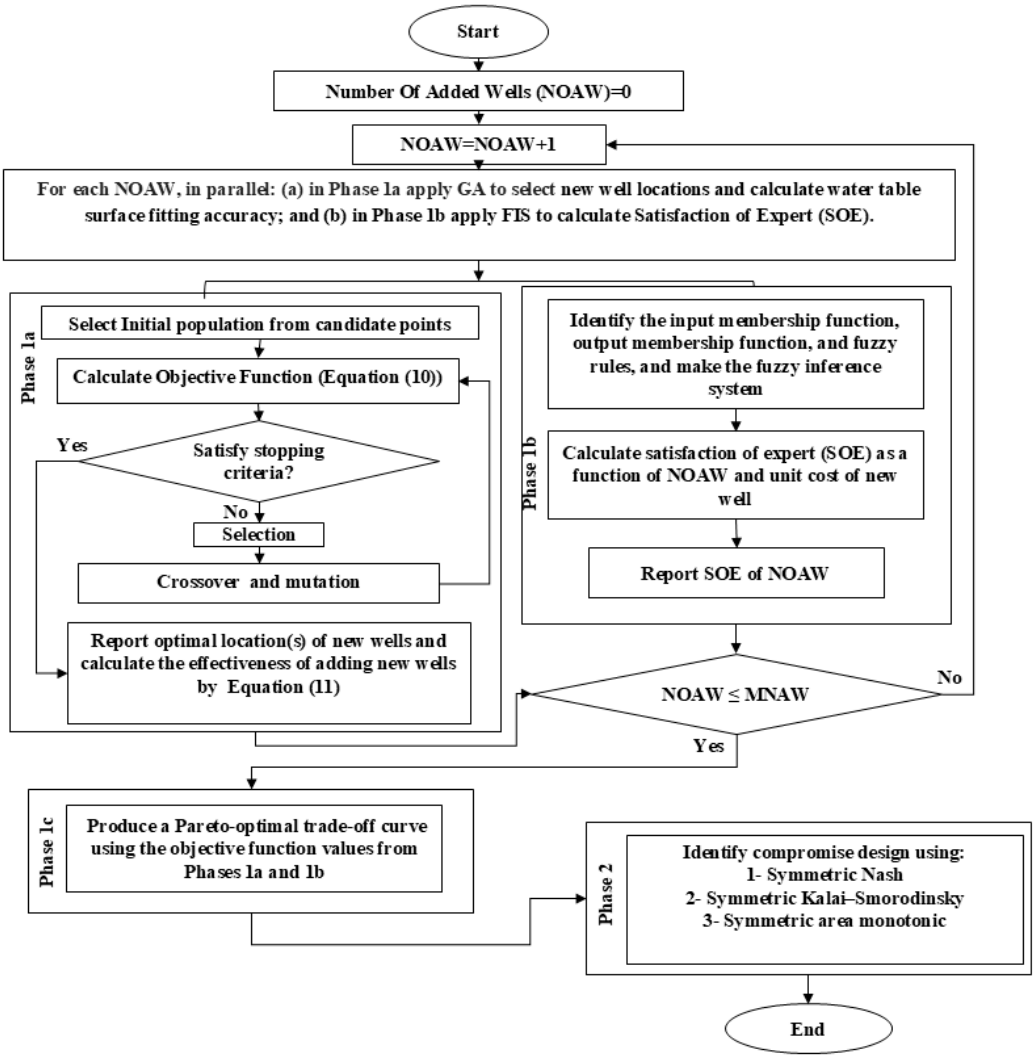

Figure 4. Algorithm for improving existing monitoring networks (NOAW: Number of Additional Observation Well(s); MNAWs: Maximum Number of Added Wells; GA: Genetic Algorithm; SOE: Satisfaction of the Expert; and FIS: Fuzzy Inference System).

2.3.1. Phase 1 (Produce Heuristic and Experiential Solutions)

Phases 1a and 1b run once for each specified Number of Additional Wells (NOAWs). NOAW values range from 1 to MNAWs (the MNAWs in this study is 12 wells). For each NOAW, within Phase 1a, a Genetic Algorithm (GA) identifies the optimal location(s) of added well(s) by maximizing the inverse of the mean sum of squared differences between the Most Accurate Interpolated Method (MAIM) and a newly kriged surface (the kriging weights change with additional well(s)). In the separate Phase 1b, a Fuzzy Inference System (FIS) calculates the Satisfaction of the Expert (SOE) for each NOAW. Phases 1a and 1b both run MNAW times. Then, Phase 1c prepares a trade-off curve reflecting tension between the results of Phases 1a and 1b.

Phase 1a (Produce and Apply Genetic Algorithm (GA))

GA is an iterative optimization technique inspired by the natural genetic processes of living organisms [49,50]. It is particularly useful for solving complex, nonlinear problems with multiple local optima, making it ideal for search and optimization tasks [7,51].

In the context of hydrology, GA excels in handling the inherent uncertainty and complexity of surface and subsurface water systems [50,52]. One of its key features is adaptability; by adjusting the mutation and crossover rates in response to changes in the

average fitness value, GA can introduce randomness to avoid local minima or increase the crossover rate for more informed reproduction when there are significant changes in fitness. This adaptability enhances its ability to find optimal solutions in dynamic and complex environments [25]. Consequently, this study employed the GA due to its proven success and widespread application in water resources, as demonstrated by [7,20]. Other optimization algorithms could substitute for the GA in the presented procedure.

The flowchart in Figure 5 illustrates the Genetic Algorithm (GA) process utilized in this study. Each optimization uses a different NOAW, ranging from one to MNAWs. In each optimization, the number of observation well(s) to be added to the existing network and the search area need to be specified. To provide the GA with feasible options, around 1000 uniformly spaced candidate well locations are provided (Figure 6). Then, the most accurate interpolation method is used to simulate groundwater levels for them.

As explained, the intent of this study was to identify the optimal locations for adding NOAW new wells to improve the accuracy of the kriged groundwater level map. To begin an optimization, the model randomly selects NOAW locations from Figure 6 candidate coordinate points. This location or set of locations can be termed a coordinate point strategy. In a NOAW 2 optimization, an individual strategy of the population of strategies identifies two new coordinate points or locations. Each location has two optimization variables, the x coordinate and y coordinate, that are adjusted within each iteration. For example, for NOAW 2, each individual has two x and two y coordinates.

Kriging is then executed using just the heads from a new monitoring network that includes the existing wells plus the NOAWs of randomly selected wells. Next, the objective function Equation (10) is used to calculate the fitness value of that monitoring network. Each optimization sought to select the NOAW location(s) that would maximize the inverse of the mean squared error difference between the kriged surface from the new monitoring network and the heads from most accurate interpolation method (MAIM) at all N locations shown in Figure 6. Each optimization stops iterating when (1) the best objective function value remains unchanged for 1000 consecutive iterations and (2) the best fitness value (BFV) is better than or equal to the best previous fitness value (BPFV). BPFV is the BFV for "NOAW-1".

$$\text{maximize } Z_{NOAW} = \left(\frac{\sum_{i=1}^{N} \left(h_i^{AIM} - h_i^{Kriged} \right)^2}{N} \right)^{-1} \quad \text{for NOAW} = 1, 2, \ldots, \text{MNAW} \quad (10)$$

In Equation (10), NOAWs is the number of additional observation wells for a particular optimization; i is the index of the center of a cell within a uniform grid covering the Qazvin Aquifer; N is the number of cells in the grid; h_i^{AIM} is the interpolated head at the *i*th location computed by the most accurate interpolation method; and h_i^{kriged} is the head at the ith location that was estimated by kriging that used heads from NOAWs and existing wells.

If the stopping criteria are not satisfied, individuals are selected using the tournament selection method to crossover parents. After crossing the parents, the new locations are replaced with the points from the search space (Figure 6) that are closest to those locations. Then, mutation occurs with a specific mutation probability.

Individual fitness values are determined (Equation (10)) and compared with the previous best fitness. If the best fitness is the same as the previous best fitness, the best repetition fitness value is increased by one; otherwise, the best fitness value is replaced with the new fitness and the counter is reset to zero. The optimization continues until both stopping criteria are met. Phase 1a ends when NOAWs equal MNAWs.

For a specified NOAW, Equation (10) minimizes the MSE of differences between the most accurately interpolated potentiometric surface elevations and newly kriged values resulting from adding new observation well(s). Equation (11) divides Root Mean Square Error (RMSE) by NOAW. If the objective function values of NOAW and NOAW-1 are equal,

the design using NOAW-1 provides the higher efficiency (Ef_{NOAW}). Thus, Ef_{NOAW} is a measure of the effectiveness per additional new well, and the larger the value, the better.

$$Ef_{NOAW} = \frac{\left(\frac{\sum_{i=1}^{N}\left(h_i^{ANN} - h_i^{kriging}\right)^2}{N}\right)^{0.5}}{NOAW} \quad (11)$$

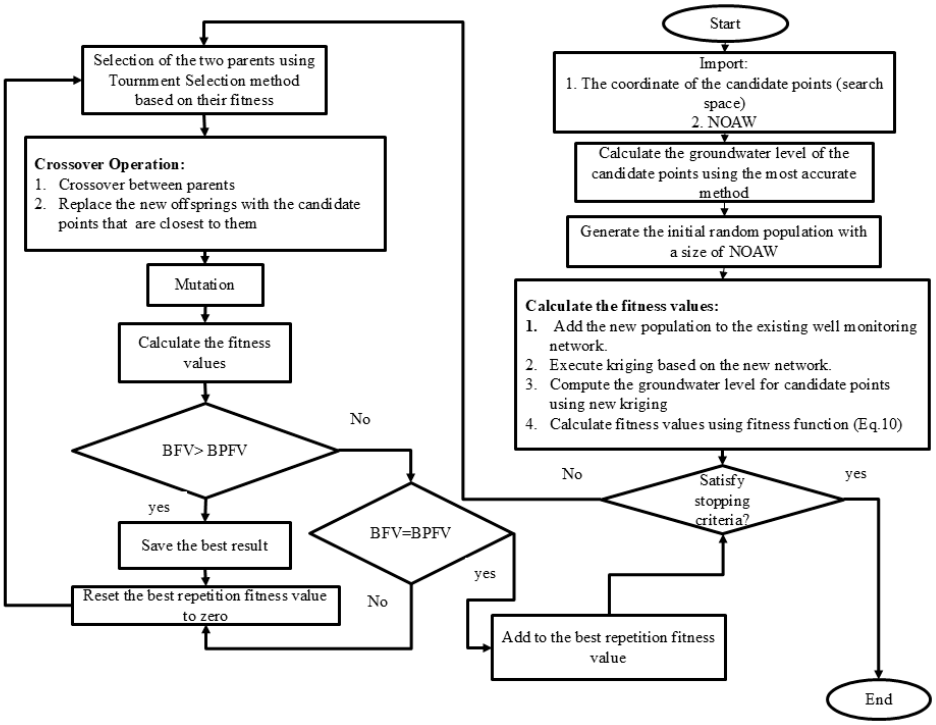

Figure 5. Flowchart of Genetic Algorithm model (BFV: the best fitness value; BPFV: the best previous fitness value).

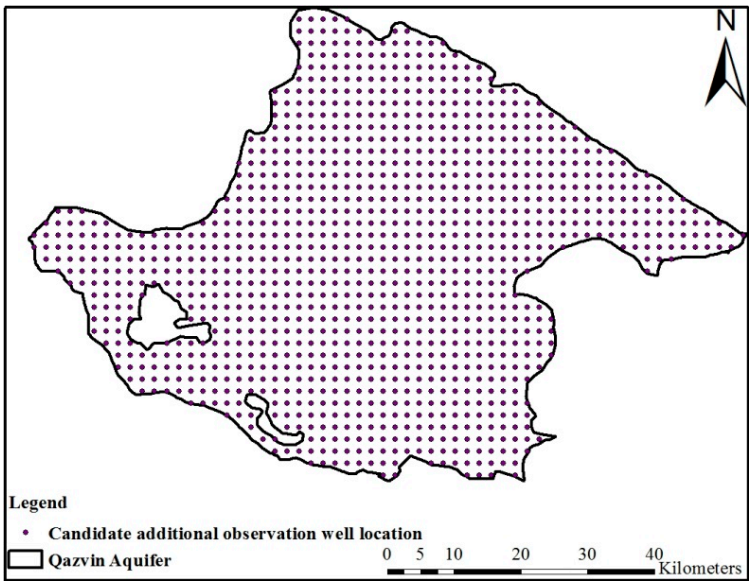

Figure 6. Qazvin Aquifer candidate additional observation well locations (search space of Genetic Algorithm).

Phase 1b (Produce and Apply Fuzzy Inference System, FIS)

Recently, fuzzy systems have been extensively utilized to address environmental issues [53,54], effectively overcoming the shortcomings of traditional methods [24,54]. Fuzzy inference supports consistent decision making using linguistic terms, similar to how decisions are made in everyday situations while remaining aligned with the principles established by the decision maker in advance. Fuzzy inference systems employ approximate reasoning, a mathematical framework developed by [55], to manage information heterogeneity and linguistic ambiguity.

The importance of incorporating an expert's knowledge in optimizing groundwater monitoring is emphasized by [24]. FIS was used in this study to achieve expert satisfaction in optimizing the monitoring network and to overcome the limitations of conventional methods. The Satisfaction of the Expert (SOE) regarding the addition of wells to the existing network is formulated using the Mamdani Fuzzy Inference System (MFIS). The MFIS was developed using the Fuzzy Logic Toolbox in MATLAB. As shown in Figure 7, the FIS consists of three main components: fuzzification, the fuzzy inference mechanism, and defuzzification.

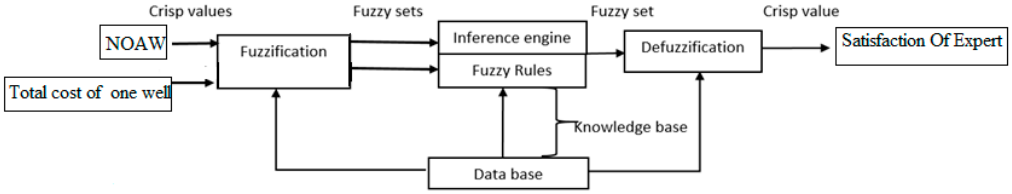

Figure 7. Fuzzy Inference System (FIS) process.

The process began assigning membership functions to all inputs and outputs and fuzzifying all variables. The Mamdani FIS in this study takes NOAWs and the unit cost of well installation as inputs and expert opinions as outputs. Figures 8–10, respectively, illustrate FIS development of membership functions for NOAWs, well installation cost, and the Satisfaction of the Expert (SOE) in the case study.

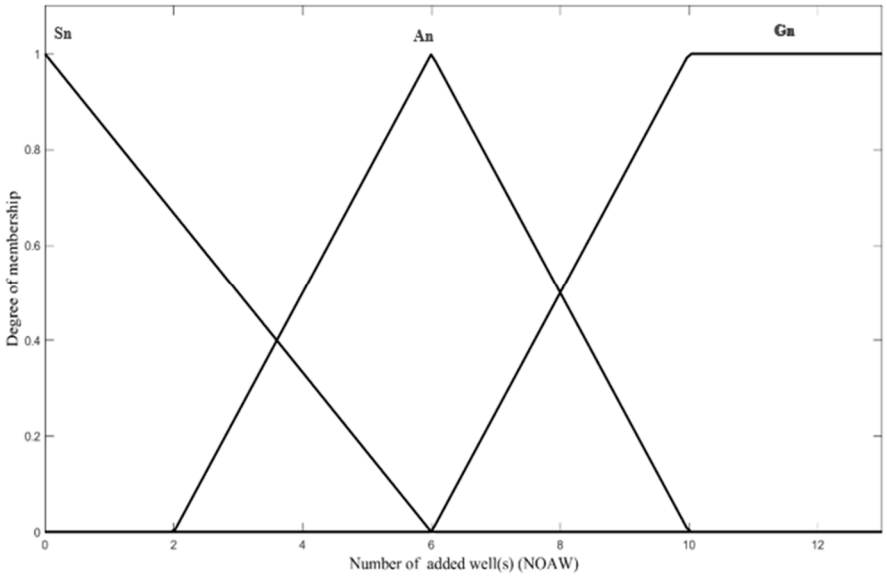

Figure 8. Membership function for NOAWs.

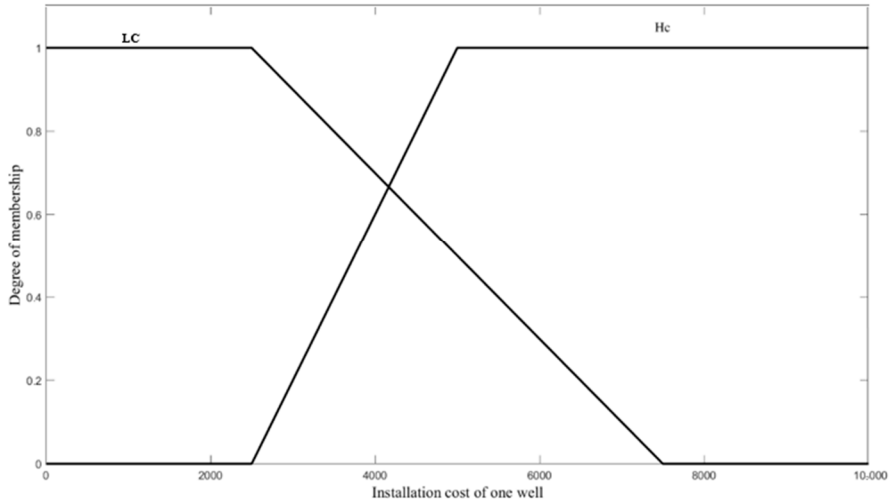

Figure 9. Membership function for installation cost of one well.

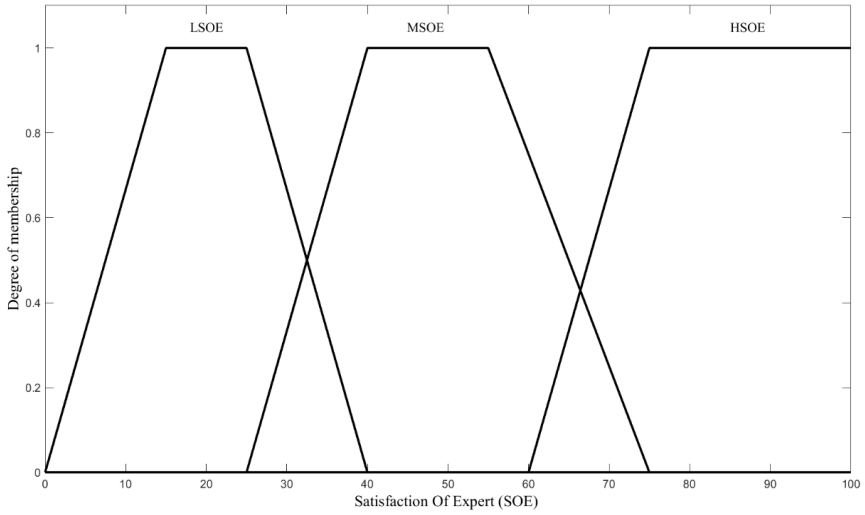

Figure 10. Membership function for satisfaction of expert.

Figure 8 shows NOAW fuzzification using triangular and trapezoidal membership functions to represent the number of monitoring wells being added: small number (Sn), average number (An), and great number (Gn). Zero wells, six wells, and from ten to twelve wells have the highest degree of memberships in groups "Sn", "An", and "Gn", respectively. The NOAWs for "Sn" changes from 0 to 5 new wells, set "An" ranges from 3 to 9 new wells, and set "Gn" ranges from 7 to 12 new wells.

Figure 9 shows unit well installation cost fuzzification into low cost (Lc) and high cost (Hc) sets, using trapezoidal membership functions. USD 0 to USD 2500 and USD 5000 and above, respectively, define membership in cost sets "LC" and "HC".

The FIS uses trapezoidal membership functions to calculate the Satisfaction of the Expert (SOE) for each NOAW (SOE_{NOAW}). Figure 10 shows the fuzzification of SOE with the number of added wells into three linguistic values: Low Satisfaction of the Expert (LSOE), Medium Satisfaction of the Expert (MSOE), and High Satisfaction of the Expert (HSOE).

After fuzzifying the variables, inference rules are applied to link the input variables to the output. Fuzzy inference is the process of formulating the mapping from a given input to an output using fuzzy logic. Table 1 presents the specific inference rules used in the developed FIS. There are three sets of inference rules that describe NOAWs and two sets that describe the unit cost of a new well, resulting in a total of six FIS model inference rules.

Table 1. Fuzzy inference system rules for determining the satisfaction of the expert with a NOAW based on the unit cost of the NOAW.

Unit Cost of New Well	NOAW		
	Small	**Average**	**Great**
Low cost	LSOE	MSOE	HSOE
High cost	MSOE	LSOE	LSOE

Then, during the inference step, these fuzzy inputs are processed using the inference operations and rules. In implementing the Mamdani approach to formulate the FIS, a maximization fuzzy operator, a minimization implication method, a maximization aggregation method, and a center of area defuzzification method are applied.

Finally, the defuzzification process converts the fuzzy output sets back into crisp values, providing a clear, actionable output. For each NOAW, the FIS application provided the SOE, effectively translating the fuzzy inputs and rules into a meaningful output that reflects expert opinions. Phase 1b ends when NOAWs equal MNAWs.

Phase 1c (Normalized Pareto Curve Production and Application)

A conflict between two objectives is quantified as the rate of change in one optimal objective value with respect to the other optimal objective value within the feasible solution space ($S \subseteq \Re^2$, where $\Re^2$ refers to two dimensions in real number space). The Phase 1a goal conflicts with the Phase 1b goal of maximizing SOE_{NOAW}. Assuming a maximization objective (in which the largest objective function value is the best), Phase 1c uses Equation (12) to normalize the optimal Ef_{NOAW} and SOE_{NOAW} values. A unit normalized value represents the best objective function value, and a zero value represents the worst.

$$O_{n,i} = \frac{O_i - O_{m,i}}{O_{x,i} - O_{m,i}} \tag{12}$$

In Equation (12), $o_{n,i}$ is the normalized ith objective function value; o_i is the ith objective function value; $o_{x,i}$ is the maximum objective value; and $o_{m,i}$ is the minimum objective value.

2.3.2. Phase 2 (Produce and Use Symmetric Conflict Resolution Methods)

To identify equilibrium or compromise solutions that consider the two objectives resulting from GA and FIS, Phase 2 applies three symmetric bargaining theory methods: (1) Nash, (2) Kalai–Smorodinsky, and (3) area monotonic. An Excel Workbook was used to calculate comparison solutions for each method.

- Method 1: Nash solution

The approach of Nash requires that a two-party conflict resolution solution satisfies four specific conditions or axioms [56,57]. As formulated in Equation (13) to address the current problem, the resulting symmetric Nash ($SOE_{NORM}{}^*$, $Ef_{NORM}{}^*$) solution lies on the Pareto frontier and maximizes the product of positive changes from the minimum feasible objective function values of the two objective functions:

$$\begin{aligned} &\text{Maximize } (SOE_{NORM} - d_1)(Ef_{NORM} - d_2) \\ &\text{Subject to the following :} \\ &d_1 \le SOE_{NORM} \le m_1 \\ &d_2 \le Ef_{NORM} = g(SOE_{NORM}) \le m_2 \end{aligned} \tag{13}$$

where Ef_{NORM} is the normalized improvement effectiveness of optimal locations selected by GA for each NOAW; SOE_{NORM} is the normalized Satisfaction of the Expert determined via MFIS for each NOAW; d_1 and d_2 are the normalized minimum acceptable objective

values; m_1 is the normalized maximum effectiveness improvement achievable according to the GA; and m_2 is the normalized maximum satisfaction of the expert achievable for the assumed new well unit cost, according to the MFIS. d_1 and d_2 equal zero (their least achievements), and m_1 and m_2 equal one (their highest achievements).

- Method 2: Kalai—Smorodinsky solution

Kalai and Smorodinsky (1975) showed that by replacing Nash's axiom of independence of irrelevant alternatives with an axiom of monotonicity, the resulting solution is monotonic and linear. Assuming a linear solution segment exists between a point of disagreement and the best point, then the best solution is at the interception of this segment with the Pareto frontier [58]. For a situation in which the mathematical optimization results and the expert's satisfaction (Ef_{NORM} = SOE_{NORM}) have equal weight, the solution of Equation (14) yields the compromise strategy in the normalized space.

$$\begin{array}{l} d_2 + \left[\frac{(m_2-d_2)}{(m_1-d_1)}\right](SOE_{NORM} - d_1) - Ef_{NORM} = 0 \\ \text{Subject to the following :} \\ d_1 \le SOE_{NORM} \le m_1 \\ Ef_{NORM} = g(SOE_{NORM}) \end{array} \quad (14)$$

Rearranging Equation (9) as $(Ef_{NORM} - d^2)/(m_2 - d_2)$ = $(SOE_{NORM} - d_1)/(m_1 - d_1)$ shows that on the line both objective function values are the same proportional distance above their minimum within their respective ranges. The compromise strategy is at the intersection of that line with the Pareto curve.

- Method 3: symmetric area monotonic solution

A solution to Nash's cooperative bargaining problem is for a linear segment starting at the disagreement point that divides the area under the curve into two subsets of equal areas [58]. The solution is the root of the nonlinear equation, as seen in Equation (15):

$$\begin{array}{c} \left[\int_{d1}^{x} g(t)dt - \frac{1}{2}(x - d_1)(g(SOE_{NORM}) + d_2)\right] \\ = \left[\int_{x}^{m1} g(t)dt - (m_1 - SOE_{NORM})d_2 + \frac{1}{2}(x - d_1)(g(SOE_{NORM}) - d_2)\right] \end{array} \quad (15)$$

3. Results

3.1. Water Table Estimation

As previously discussed, the accuracies of the four surface fitting methods for the Qazvin Aquifer were evaluated. This process commenced by partitioning the total observed head and location data into separate training and testing datasets. Subsequently, each of the four methods underwent training using the identical training dataset and testing using the same testing dataset. A comparative analysis of the performance of each method is presented in Table 2.

Table 2. Testing cross-validation results of the best of each surface fitting method.

Statistical Parameter	Method							
	IDW		Kriging		MLP-ANN		Spline	
	Train	Test	Train	Test	Train	Test	Train	Test
R^2	1.00	0.75	1.00	0.81	0.97	0.93	1.00	0.79
RMSE	0.09	26.80	0.00	24.53	10.77	13.70	0.04	26.52
MAE	0.04	13.44	0.00	11.93	4.50	6.62	0.02	12.10
RMSLE	0.000	0.009	0.000	0.009	0.004	0.005	0.000	0.009
ARE	0.001	0.496	0.000	0.423	0.155	0.279	0.001	0.457

The results indicated that the MLP-ANN provided the most accurate estimation of groundwater levels at testing locations, while ensuring that no water table heads were estimated above the ground surface. This was evidenced by its highest R^2 value and lowest RMSE, MAE, RMSLE, and ARE values in the test dataset. In addition to our findings, refs. [8,59] also demonstrated that the ANN method had the best performance in their studies. Their results corroborated our conclusion that machine learning excels in predictive accuracy and generalization capability, further reinforcing our favorable conclusion concerning the effectiveness of this method for groundwater level predictions.

The optimal MLP-ANN structure comprised a feed-forward neural network with two hidden layers, featuring 6 and 33 neurons, respectively. Sigmoid tangent activation functions were employed in the hidden layers, while a linear transfer function was used in the output layer. Consequently, Phase 1a utilized this MLP-ANN to estimate groundwater levels at candidate locations for adding well(s).

Kriging demonstrated the highest accuracy after MLP-ANN. However, it incorrectly produced some water table heads above the ground surface. Regardless of its accuracy, kriging requires defining the spatial correlation structure using a parameterized but unknown variogram model. This process is complicated and requires making numerous assumptions, such as stationarity, isotropy, and multivariable normality. These conditions are not easily verifiable and require expert knowledge of spatial statistics. Another study noted that the accuracy of kriging can be significantly affected by the assumptions and conditions needed for its implementation [6,14]. Their simulated data followed a Gaussian distribution with a specified variogram model, likely contributing to kriging's minimal prediction error in that context.

By applying MLP-ANN, the data do not need to assume a specific distribution, and more input data can be used to increase accuracy. The training process is also more flexible, and various methods can be utilized to enhance accuracy and control error, as demonstrated in this study. Additionally, the spatial relationships between hydrogeological variables are poorly understood due to their inherent complexity and nonlinearity. Therefore, integrating soft computing models with each other or with numerical methods (creating hybrid models) significantly enhances our comprehension of these intricate relationships. This approach leads to superior modeling accuracy, as previously demonstrated [25,52].

Here, the best kriging option used a Gaussian distribution semivariogram, which was then applied in Phase 1a. While both IDW and spline methods showed good training results, they did not generalize as effectively as MLP-ANN and kriging. In line with that, [60,61] showed that kriging was more accurate than IDW, and the spline was less accurate compared to kriging was shown by [62,63]

3.2. Phase 1a (GA Application)

Because MLP-ANN most closely matched observed heads during testing, the purpose of this phase is to cause kriged heads to match more closely the MLP-ANN heads for GA-selected locations. To execute the designed GA, a code has been written in MATLAB 2016a.

Within each optimization, the GA provides the locations of the NOAW wells that will most improve the overall accuracy of the kriged surface. The red line in Figure 11 shows the change in RMSE as new wells are added. As demonstrated, RMSE decreases as the number of added wells increases. The RMSE for each NOAW was lower than the RMSE from the previous iteration, demonstrating that the algorithm's performance improved as it progressed. Without adding a new well, the RMSE was 20.42 m. By adding wells, the improvement in RMSE ranged from 0.73 m for one well to 2 m for twelve wells.

Figure 11 illustrates the effectiveness per added well (Ef_{NOAW}), computed by Equation (11), versus RMSE. Increasing NOAWs to improve accuracy (by decreasing RMSE), asymptotically decreased the per-well effectiveness (Ef_{NOAW}). Adding one well had the most significant impact compared to other NOAW scenarios. However, as more wells were added, the intensity of RMSE change fluctuated. For example, the change in

RMSE for one well was 3.56%. For four wells, it was 0.1%, and it increased to 0.45% for six wells. Then, it started to decrease again, and for twelve wells, the RMSE increased by 1.40%. The effectiveness changes also decreased, similar to the trend in RMSE. A significant change was observed with the addition of the first well, about 50%, and from NOAW 10 onwards, the effectiveness remained almost constant. The initial result was presented at the 12th International Conference on Hydro Informatics [64]. A similar trend and concerns were observed in the study by [5].

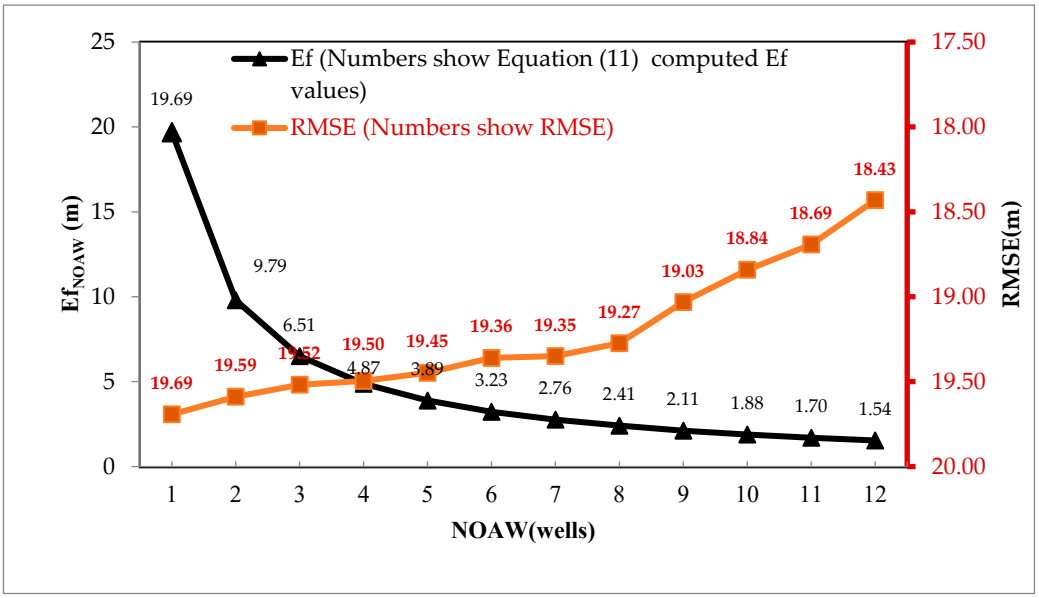

Figure 11. Ef and RMSE as functions of NOAWs.

A trade-off between increasing accuracy and efficiency occurred at NOAW 5, where the lines intersected. In other words, a designer can determine the number of wells to add by considering the intersection of two lines as well as the percent change in efficiency resulting from adding an additional well. Decision making can be aided by considering the trade-off between accuracy and efficiency in adding wells.

Although the GA is designed to find the optimal locations for NOAWs to improve accuracy, Figure 11 shows that the amount of improvement becomes less significant or even increases slightly in some cases. This suggests that adding more wells might not always be cost-effective, as the change in RMSE diminishes with additional wells. Following this section, we demonstrated how the application of FIS can enable experts' opinions to assist decision making further.

3.3. Phase 1b (FIS Application)

To address the concerns mentioned in the previous section and to overcome the limitations of using only conventional methods for hydrologic decision making, an MFIS was developed [24]. In this MFIS, NOAWs and the unit cost of well installation were considered to evaluate expert satisfaction and incorporate expert opinions into the optimization process. The proposed model is flexible enough to incorporate additional information that could impact expert opinions concerning their satisfaction. However, in this study, we focused on demonstrating how considering only the cost and NOAWs can involve decision makers in the numerical optimization model.

Figure 12 demonstrates the inference mechanism for specific inputs, such as NOAW 9, and a unit well cost of USD 4000. This figure illustrates how the features are applied to map the input variables to the output. The MFIS was run for three different well costs, as presented in Table 3. The result showed that as the cost increased, expert satisfaction decreased. The proposed model utilized the result of MFIS for a cost of USD 4000.

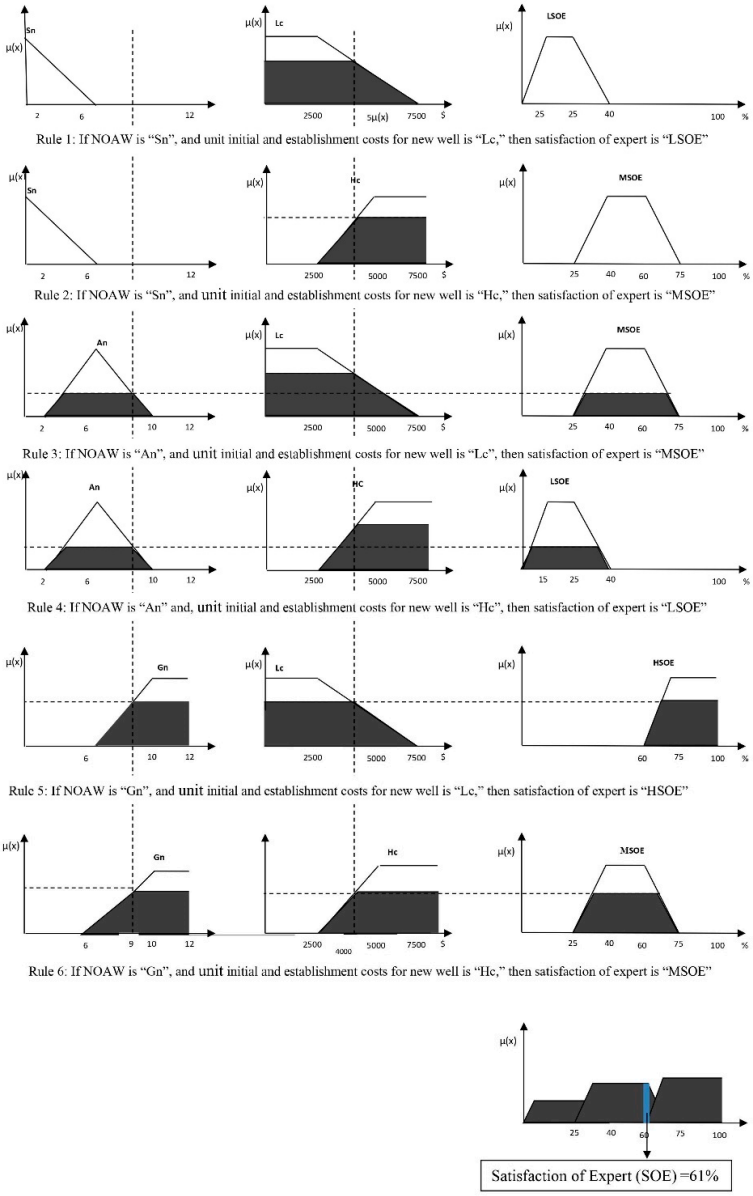

Figure 12. Fuzzification, inference, and defuzzification processes in determining the Satisfaction of the Expert (SOE) for each NOAW (for NOAWs = 9 and unit well cost = USD 4000, SOE = 61%).

Table 3. Satisfaction of the expert (SOE) with each NOAW, as a function of unit well installation cost.

Number of Additional Wells (NOAWs)	Satisfaction of the Expert (SOE) for USD 4000/Well	Satisfaction of the Expert (SOE) for USD 6000/Well	Satisfaction of the Expert (SOE) for USD 8000/Well
1	35	44	49
2	36	44	49
3	37	42	43
4	37	31	31
5	39	27	24
6	39	25	20
7	44	27	20
8	52	30	20
9	61	27	20
10	68	25	20
11	68	25	20
12	68	25	20

For a unit well cost of USD 4000, the results showed that increasing NOAWs led to an increase in expert satisfaction. However, the amount of SOE remained constant from NOAW 10 onwards. To combine the results from both Phases 1a and 1b, conflict resolution methods were applied.

3.4. Phase 1c (Pareto Curve Production)

In this step, the application of Equation (11) to the results from Phases 1a and 1b produces a Pareto curve (Figure 13). Figure 13 Pareto curve does not show values for NOAWs of 4, 6, 11, and 12 because they are inferior to adjacent solutions for NOAWs 3, 5, and 10, respectively (they have the same SOE_{NOAW} but a smaller Ef_{NOAW} than an adjacent solution). In Figure 10, the normalized point $(d_1, d_2) \in R^2$ has the worst possible payoff values for both objectives. The best normalized SOE and Ef values are, respectively, at points (m_1, d_2) and (d_1, m_2). The equation assigned a value of 1 to the best result from each phase and a value of 0 to the worst result for both phases. Graphically, human supporters of a particular strategy often want their achieved objective function value to be as much above d_1 and d_2 as possible. Incorporating expert opinions into the results, initially suggested solely based on the GA, highlighted how integrating expert input can lead to more feasible and practical solutions.

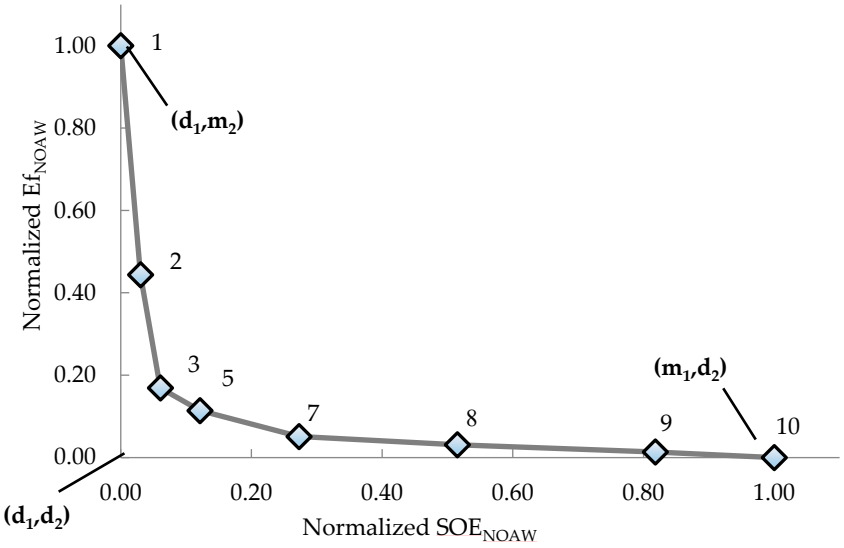

Figure 13. Normalized Pareto optimum curve of Ef versus SOE for USD 4000 unit well cost (labels show NOAWs).

3.5. Phase 2

To find the equilibrium strategies, three bargaining theory methods were used. The symmetric Nash, symmetric Kalai–Smorodinsky, and the symmetric area monotonic methods, respectively, specified eight, five, and five wells as the compromise numbers of wells to add (NOAWs) to the Qazvin Aquifer monitoring network. Figure 14 shows kriged groundwater contour maps prepared for each compromise strategy. Each map employed existing wells plus the NOAW wells specified by the bargaining game. The average design recommendation of the three Phase 2 gaming methods was six wells. However, a five-well solution dominates over a six-well solution (they have the same $SOE_{NOAW,}$ but a five-well solution has a greater Ef_{NOAW} than a six-well solution).

Otherwise, because conflict resolution aims to find a state where all objectives are acceptably satisfied, strategies having a Ef_{NORM}/SOE_{NORM} ratio that is close to 1 in normalized space is preferable. A ratio close to one showed that both objectives are close to equally achieved. A five-well NOAW strategy yielded an Ef_{NORM}/SOE_{NORM} value closest to 1. The symmetric Kalai–Smorodinsky and the symmetric area monotonic picked the optimal compromise NOAWs. Therefore, adding five wells to the aquifer is recommended

to the water agency. This study reveals that FIS is a reliable tool for integrating expert opinions into mathematics and statistical methods for optimizing monitoring networks. This finding is consistent with the results of [53,65] that underscore the effectiveness of FIS in enhancing decision making processes.

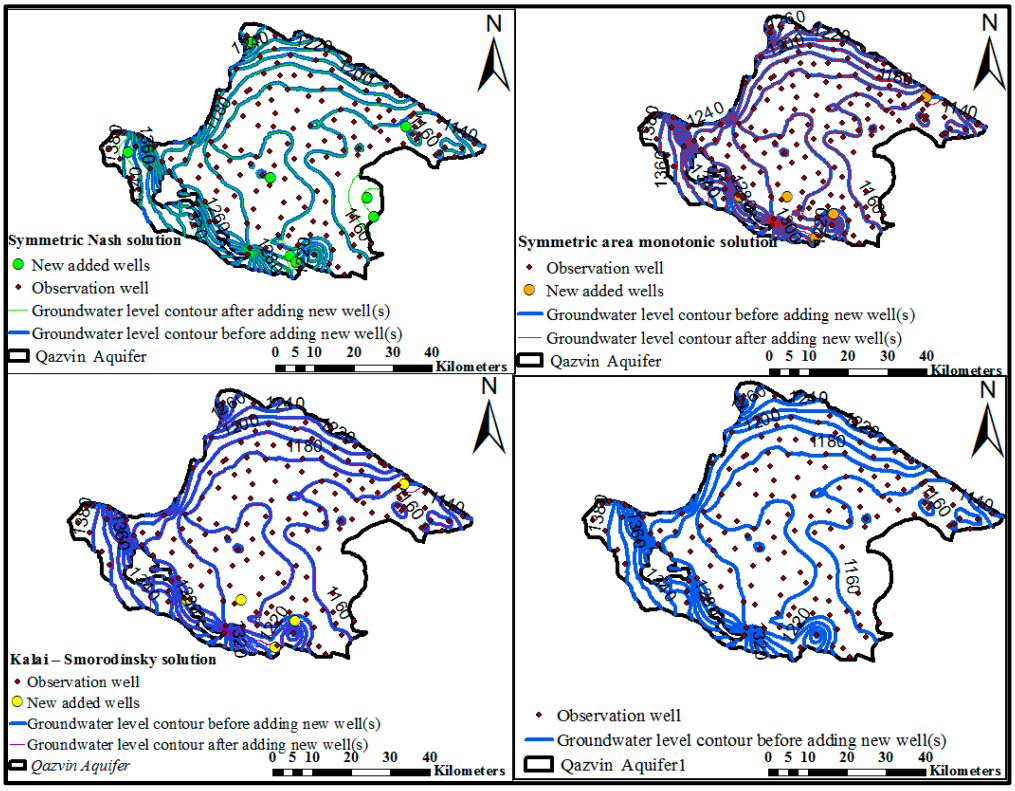

Figure 14. The groundwater level contour maps based on bargaining game results.

Regarding the results of the three bargaining methods, five and eight observation wells were selected to be added to the aquifer. The five wells are mainly distributed along the southern boundary of the aquifer. Most of the southern aquifer relies on groundwater as the primary water resource for the agricultural sector and does not have a significant surface water supply. The study by [66] showed that this region, where most observation wells are added, experiences more severe drought during drought years than other parts of the aquifer, leading to significant fluctuations in water levels and thus requiring more wells for monitoring. Additionally, kriging showed greater error near the aquifer's boundaries due to a lack of known data points in these areas, particularly in the southern part. This suggests that the GA successfully identified optimal locations to support kriging, thereby enhancing the accuracy of groundwater level predictions.

However, when the number of wells increases beyond five, some wells are also added to the center of the aquifer, where the groundwater is more stable than at the boundary. Regardless of the number of added wells, the areas that show severe drought consistently remain the priority for well placement. When the number of added wells is lower, they are mostly placed in areas with more significant water level fluctuations. As the number increases, the locations extend to other parts of the aquifer that are not as variable.

4. Discussion

A novel approach to monitoring network expansion is presented here that uses encapsulated fuzzy expert opinions to negotiate between quantitative results from artificial intelligence-guided optimization and fuzzy expert opinions. A methodology was developed in the present study to address Rosen's statement [24] that expert opinion information and mathematical–statistical information ought to be incorporated simultaneously into the

development of a potentiometric surface monitoring well network. First, the evaluation shows that MLP-ANN produces more accurate potentiometric surface maps than spline, IDW, and the commonly used kriging. Accordingly, the methodology provides a guide to the placement of new observation wells so that kriging values will become more like those generated by MLP-ANN. In order to minimize the total difference between heads from kriging and heads from MLP-ANN, the Genetic Algorithm (GA) optimization determines the locations of new observation wells for each set of candidate new observation wells. Results from the GA showed that the rate of decreasing RMSE per additional well decreases as NOAWs increase. Decision makers can select one of two criteria to decide when to stop adding wells: minimum acceptable RMSE and minimum acceptable RMSE reduction per well. Efficiency and accuracy of intersection lines can also be critical factors in choosing NOAWs that balance both.

Along with the optimization process, a Fuzzy Inference System (FIS) is created by incorporating the opinions of local experts regarding well installation costs and the practical number of monitoring wells to be installed. The MFIS quantifies the Satisfaction of the Expert with each possible number of new monitoring wells up to 12.

In their determination of the optimal number of new wells, GA and FIS differ. The conflict is resolved by utilizing three game theory symmetric techniques (Nash, Kalai–Smorodinsky, and area monotonic) after preparing a normalized Pareto optimum curve. In their respective approaches, the three approaches suggest adding eight, five, and five monitoring wells. On average, the three approaches propose six monitoring wells. According to Figure 13, the six-well design is inferior and dominated by the five-well design; therefore, the average of the bargaining methods for a six-well design is five wells.

The limitation of the model in the context of application to other situations lies in its computational complexity, especially when scaling up for very large problems. As the number of wells increases, this complexity could require significant processing power and time. The time required to tune and train an artificial neural network increases with network complexity and the volume of data. Without access to advanced CPU or GPU technology, these limitations could hinder the application [6].

Future work should focus on several key areas to enhance the transferability and applicability of the model. Assigning weights to additional observation candidates based on their perceived importance, particularly in areas experiencing severe declines in groundwater levels, could provide increased accuracy in those areas. Incorporating the location of the new well(s) into the Fuzzy Inference System (FIS) is another potential enhancement. Exploring alternative metaheuristic algorithms and evaluating their impact on the optimization process, especially when adding many wells, could further improve the model's effectiveness and efficiency.

In summary, a novel technique is presented to predict where and how many observation wells should be installed to improve the accuracy of groundwater level monitoring networks. Both sophisticated computational results and critically important situation-specific hydrogeologic and other field experiences are appropriately considered in this technique. The developed algorithm is designed to be easily upgraded to suit the contexts of other areas. Additionally, these hybrid technologies can also be adapted to map other variables such as groundwater quantity, soil sensors, climatology stations, and other sampling data.

Author Contributions: Conceptualization, M.H. and R.C.P.; methodology, M.H. and R.C.P.; software, M.H. and R.C.P.; validation, M.H., R.C.P., and M.Y.; formal analysis, M.H. and R.C.P.; investigation, M.H. and R.C.P.; resources, R.C.P. and M.Y.; data curation, M.H.; writing—original draft preparation, M.H. and R.C.P.—review and editing, M.H., R.C.P., and M.Y.; visualization, M.H., R.C.P., and M.Y.; supervision, R.C.P. and M.Y.; project administration, R.C.P. and M.Y.; funding acquisition, M.H. and R.C.P. All authors have read and agreed to the published version of the manuscript.

Funding: This research was funded by Qazvin Regional Water Company 2019, grant number 95/28590/101, and Utah Agricultural Experiment Station 2019, grant number UAES #9210.

Data Availability Statement: The dataset can be found at http://www.hydroshare.org/resource/84bf350e46de412fbf09a69369f4a686 (accessed on 15 May 2024).

Conflicts of Interest: The authors declare no conflicts of interest. The funders had no role in the design of the study; in the collection, analyses, or interpretation of data; in the writing of the manuscript; or in the decision to publish the results.

References

1. Rajaee, T.; Ebrahimi, H.; Nourani, V. A Review of the Artificial Intelligence Methods in Groundwater Level Modeling. *J. Hydrol.* **2019**, *572*, 336–351. [CrossRef]
2. Amiri, S.; Rajabi, A.; Shabanlou, S.; Yosefvand, F.; Izadbakhsh, M.A. Prediction of Groundwater Level Variations Using Deep Learning Methods and GMS Numerical Model. *Earth Sci. Inform.* **2023**, *16*, 3227–3241. [CrossRef]
3. Todd, D.K.; Mays, L.W. *Groundwater Hydrology*; John Wiley & Sons: Hoboken, NJ, USA, 2005; ISBN 0471452548.
4. Narany, T.S.; Ramli, M.F.; Aris, A.Z.; Sulaiman, W.N.A.; Fakharian, K. Spatial Assessment of Groundwater Quality Monitoring Wells Using Indicator Kriging and Risk Mapping, Amol-Babol Plain, Iran. *Water* **2014**, *6*, 68–85. [CrossRef]
5. Kavusi, M.; Khashei Siuki, A.; Dastourani, M. Optimal Design of Groundwater Monitoring Network Using the Combined Election-Kriging Method. *Water Resour. Manag.* **2020**, *34*, 2503–2516. [CrossRef]
6. Tavassoli, A.; Waghei, Y.; Nazemi, A. Comparison of Kriging and Artificial Neural Network Models for the Prediction of Spatial Data. *J. Stat. Comput. Simul.* **2022**, *92*, 352–369. [CrossRef]
7. Majedi-Asl, M.; Fuladipanah, M.; Mahmoudpour, H.; Ebrahimpour, E.; Kisi, O. Optimization Design of Quality Monitoring Network of Urmia Plain Using Genetic Algorithm and Vulnerability Map. *Geocarto Int.* **2023**, *38*, 2152492. [CrossRef]
8. Abdi, E.; Ali, M.; Santos, C.A.G.; Olusola, A.; Ghorbani, M.A. Enhancing Groundwater Level Prediction Accuracy Using Interpolation Techniques in Deep Learning Models. *Groundw. Sustain. Dev.* **2024**, *26*, 101213. [CrossRef]
9. Uyan, M.; Cay, T. Spatial Analyses of Groundwater Level Differences Using Geostatistical Modeling. *Environ. Ecol. Stat.* **2013**, *20*, 633–646. [CrossRef]
10. Rabah, F.K.J.; Ghabayen, S.M.; Salha, A.A. Effect of GIS Interpolation Techniques on the Accuracy of the Spatial Representation of Groundwater Monitoring Data in Gaza Strip. *J. Environ. Sci. Technol.* **2011**, *4*, 579–589. [CrossRef]
11. Amini, H.; Ashrafzadeh, A.; Khaledian, M. Enhancing Groundwater Salinity Estimation through Integrated GMDH and Geostatistical Techniques to Minimize Kriging Interpolation Error. *Earth Sci. Inform.* **2024**, *17*, 283–297. [CrossRef]
12. Jithendra, T.; Basha, S.S. Analyzing Groundwater Level with Hybrid ANN and ANFIS Using Metaheuristic Optimization. *Earth Sci. Inform.* **2023**, *16*, 3323–3353. [CrossRef]
13. Hashemi, M.; Sepaskhah, A.R. Evaluation of Artificial Neural Network and Penman–Monteith Equation for the Prediction of Barley Standard Evapotranspiration in a Semi-Arid Region. *Theor. Appl. Climatol.* **2020**, *139*, 275–285. [CrossRef]
14. Tirol Kirçiçek, N.; Baba, A.; Koçbay, A.; Toklu, M.M. Evaluation of GIS-Based Spatial Interpolation Methods for Groundwater Level: A Case Study of Türkiye. *Turk. J. Earth Sci.* **2024**, *33*, 576–591. [CrossRef]
15. Aceves-De-Alba, J.; ENRIQUE Júnez, H.; González-Trinidad, J.; Cardona-Benavides, A.; Bautista-Capetillo, C. Methodology for the Optimization of Groundwater Quality Monitoring Networks Oriented to Satisfy a Specific Spatial Coverage. *Appl. Ecol. Environ. Res.* **2019**, *17*, 10861–10882. [CrossRef]
16. Nunes, L.M.; Cunha, M.C.; Ribeiro, L. Groundwater Monitoring Network Optimization with Redundancy Reduction. *J. Water Resour. Plan. Manag.* **2004**, *130*, 33–43. [CrossRef]
17. Ohmer, M.; Liesch, T.; Wunsch, A. Spatiotemporal Optimization of Groundwater Monitoring Networks Using Data-Driven Sparse Sensing Methods. *Hydrol. Earth Syst. Sci.* **2022**, *26*, 4033–4053. [CrossRef]
18. Abedian, H.; Mohammadi, K.; Rafiee, R. Optimizing Monitoring Network of Water Table by Geostatistical Methods. *J. Geol. Min. Res.* **2013**, *5*, 223–231. [CrossRef]
19. Teimoori, S.; Olya, M.H.; Miller, C.J. Groundwater Level Monitoring Network Design with Machine Learning Methods. *J. Hydrol.* **2023**, *625*, 130145. [CrossRef]
20. Mirzaie-Nodoushan, F.; Bozorg-Haddad, O.; Loaíciga, H.A. Optimal Design of Groundwater-Level Monitoring Networks. *J. Hydroinform.* **2017**, *19*, 920–929. [CrossRef]
21. Ayvaz, M.T.; Elçi, A. Identification of the Optimum Groundwater Quality Monitoring Network Using a Genetic Algorithm Based Optimization Approach. *J. Hydrol.* **2018**, *563*, 1078–1091. [CrossRef]
22. Hosseini, M.; Kerachian, R. A Data Fusion-Based Methodology for Optimal Redesign of Groundwater Monitoring Networks. *J. Hydrol.* **2017**, *552*, 267–282. [CrossRef]
23. Amiri, H.; Azadi, S.; Javadpour, S.; Naghavi, A.A.; Boczkaj, G. Selecting Wells for an Optimal Design of Groundwater Monitoring Network Based on Monitoring Priority Map: A Kish Island Case Study. *Water Resour. Ind.* **2022**, *27*, 100172. [CrossRef]
24. Rosen, M.R. Groundwater monitoring networks, in Groundwater. In *Encyclopedia of Life Support Systems (EOLSS)*; Silveira, L., Ed.; Eolss Publishers: Oxford, UK, 2003; Available online: https://www.eolss.net/ebooklib/bookinfo/groundwater.aspx#chapters (accessed on 15 May 2024).
25. Kraft, B.; Jung, M.; Körner, M.; Reichstein, M. Hybrid Modeling: Fusion of a Deep Approach and Physics-Based Model for Global Hydrological Modeling. *Int. Arch. Photogramm. Remote Sens. Spat. Inf. Sci.* **2020**, *43*, 1537–1544. [CrossRef]

26. Fisher, J. *Optimization of Water-Level Monitoring Networks in the Eastern Snake River Plain Aquifer Using a Kriging-Based Genetic Algorithm Method*; Scientific Investigations Report 2013-5120; US Geological Survey: Reston, VA, USA, 2013.
27. Firat, M.; Turan, M.E.; Yurdusev, M.A. Comparative Analysis of Fuzzy Inference Systems for Water Consumption Time Series Prediction. *J. Hydrol.* **2009**, *374*, 235–241. [CrossRef]
28. Mamdani, E.H.; Assilian, S. An Experiment in Linguistic Synthesis with a Fuzzy Logic Controller. *Int. J. Hum. Comput. Stud.* **1973**, *51*, 135–147. [CrossRef]
29. Takagi, T.; Sugeno, M. Fuzzy Identification of Systems and Its Applications to Modeling and Control. *IEEE Trans. Syst. Man Cybern.* **1985**, *1*, 116–132. [CrossRef]
30. Dhar, A.; Patil, R.S. Multiobjective Design of Groundwater Monitoring Network Under Epistemic Uncertainty. *Water Resour. Manag.* **2012**, *26*, 1809–1825. [CrossRef]
31. Masoumi, Z.; Rezaei, A.; Maleki, J. Improvement of Water Table Interpolation and Groundwater Storage Volume Using Fuzzy Computations. *Environ. Monit. Assess.* **2019**, *191*, 401. [CrossRef]
32. Nourani, V.; Maleki, S.; Najafi, H.; Baghanam, A.H. A Fuzzy Logic-Based Approach for Groundwater Vulnerability Assessment. *Environ. Sci. Pollut. Res.* **2024**, *31*, 18010–18029. [CrossRef]
33. Noori, R.; Maghrebi, M.; Mirchi, A.; Tang, Q.; Bhattarai, R.; Sadegh, M.; Noury, M.; Haghighi, A.T.; Kløve, B.; Madani, K. Anthropogenic Depletion of Iran's Aquifers. *Proc. Natl. Acad. Sci. USA* **2021**, *118*, e2024221118. [CrossRef]
34. Moridi, A. State of Water Resources in Iran. *Int. J. Hydrol.* **2017**, *1*, 111–114. [CrossRef]
35. Hashemi, M.; Zadeh, H.M.; Zarghami, M.; Demeke, B.W.; Delgarm, R.T. An Analysis of Why Rehabilitation and Balancing Programs for Aquifers Do Not Meet Water Organizations' Targets (a Case Study of the Qazvin Aquifer in Iran). *Agric. Water Manag.* **2023**, *281*, 108258. [CrossRef]
36. Yao, L.; Huo, Z.; Feng, S.; Mao, X.; Kang, S.; Chen, J.; Xu, J.; Steenhuis, T.S. Evaluation of Spatial Interpolation Methods for Groundwater Level in an Arid Inland Oasis, Northwest China. *Environ. Earth Sci.* **2014**, *71*, 1911–1924. [CrossRef]
37. Mair, A.; Fares, A. Comparison of Rainfall Interpolation Methods in a Mountainous Region of a Tropical Island. *J. Hydrol. Eng.* **2011**, *16*, 371–383. [CrossRef]
38. Ohmer, M.; Liesch, T.; Goeppert, N.; Goldscheider, N. On the Optimal Selection of Interpolation Methods for Groundwater Contouring: An Example of Propagation of Uncertainty Regarding Inter-Aquifer Exchange. *Adv. Water Resour.* **2017**, *109*, 121–132. [CrossRef]
39. Boumpoulis, V.; Michalopoulou, M.; Depountis, N. Comparison between Different Spatial Interpolation Methods for the Development of Sediment Distribution Maps in Coastal Areas. *Earth Sci. Inform.* **2023**, *16*, 2069–2087. [CrossRef]
40. Franke, R. Smooth Interpolation of Scattered Data by Local Thin Plate Splines. *Comput. Math. Appl.* **1982**, *8*, 273–281. [CrossRef]
41. Mitáš, L.; Mitášová, H. General Variational Approach to the Interpolation Problem. *Comput. Math. Appl.* **1988**, *16*, 983–992. [CrossRef]
42. Safavi, H.R.; Ahmadi, K.M. Prediction and Assessment of Drought Effects on Surface Water Quality Using Artificial Neural Networks: Case Study of Zayandehrud River, Iran. *J. Environ. Health Sci. Eng.* **2015**, *13*, 68. [CrossRef]
43. Lophaven, S.N.; Nielsen, H.B.; Sondergaard, J.; Dace, A. *A Matlab Kriging Toolbox*; Technical Report No. IMM-TR-2002-12; Technical University of Denmark: Copenhagen, Denmark, 2002.
44. Tomassi, A.; Trippetta, F.; de Franco, R.; Ruggieri, R. From Petrophysical Properties to Forward-Seismic Modeling of Facies Heterogeneity in the Carbonate Realm (Majella Massif, Central Italy). *J. Pet. Sci. Eng.* **2022**, *211*, 110242. [CrossRef]
45. Shexo, A.H.M.; Abdullah, T.H. Robust Estimation Based on Lognormal Kriging Technique for Some Soil Data. *Math. Model. Eng. Probl.* **2024**, *11*, 5. [CrossRef]
46. Rajabi, F.; Faraji, N.; Hashemi, M. An Efficient Video-Based Rainfall Intensity Estimation Employing Different Recurrent Neural Network Models. *Earth Sci. Inform.* **2024**, *17*, 2367–2380. [CrossRef]
47. Shadkani, S.; Hashemi, S.; Pak, A.; Lahijan, A.B. Random Forest and Multilayer Perceptron Hybrid Models Integrated with the Genetic Algorithm for Predicting Pan Evaporation of Target Site Using a Limited Set of Neighboring Reference Station Data. *Earth Sci. Inform.* **2024**, *17*, 1261–1280. [CrossRef]
48. Mirarabi, A.; Nassery, H.R.; Nakhaei, M.; Adamowski, J.; Akbarzadeh, A.H.; Alijani, F. Evaluation of Data-Driven Models (SVR and ANN) for Groundwater-Level Prediction in Confined and Unconfined Systems. *Environ. Earth. Sci.* **2019**, *78*, 489. [CrossRef]
49. Magalhães-Mendes, J. A Comparative Study of Crossover Operators for Genetic Algorithms to Solve the Job Shop Scheduling Problem. *WSEAS Trans. Comput.* **2013**, *12*, 164–173.
50. Mahmoudpour, H.; Janatrostami, S.; Ashrafzadeh, A. Optimal Design of Groundwater Quality Monitoring Network Using Aquifer Vulnerability Map. *Water Resour. Manag.* **2023**, *37*, 797–818. [CrossRef]
51. Hashemi, M.; Mazandarani Zadeh, H.; Daneshkare Arasteh, P.; Zarghami, M. Economic and Environmental Impacts of Cropping Pattern Elements Using Systems Dynamics. *Civ. Eng. J.* **2019**, *5*, 1020–1032. [CrossRef]
52. Gladish, D.W.; Pagendam, D.E.; Janardhanan, S.; Gonzalez, D. Geostatistical Based Optimization of Groundwater Monitoring Well Network Design. *Front. Earth Sci.* **2023**, *11*, 1188316. [CrossRef]
53. Loganathan, S.; Ramakrishnan, D.; Sathiyamoorthy, M.; Azamathulla, H.M. Assessment of Irrigational Suitability of Groundwater in Thanjavur District, Southern India Using Mamdani Fuzzy Inference System. *Results Eng.* **2024**, *21*, 101789. [CrossRef]
54. Kambalimath, S.; Deka, P.C. A Basic Review of Fuzzy Logic Applications in Hydrology and Water Resources. *Appl. Water Sci.* **2020**, *10*, 191. [CrossRef]

55. Zadeh, L.A. Fuzzy Sets. *Inf. Control.* **1965**, *8*, 338–353. [CrossRef]
56. Nash, J.F. The Bargaining Problem. *Econometrica* **1950**, *18*, 155–162. [CrossRef]
57. Kalai, E.; Smorodinsky, M. Other Solutions to Nash's Bargaining Problem. *Econometrica* **1975**, *43*, 513–518. [CrossRef]
58. Salazar, R.; Szidarovszky, F.; Coppola, E.; Rojano, A. Application of Game Theory for a Groundwater Conflict in Mexico. *J. Environ. Manag.* **2007**, *84*, 560–571. [CrossRef]
59. Chitsazan, M.; Rahmani, G.; Neyamadpour, A. Groundwater Level Simulation Using Artificial Neural Network: A Case Study from Aghili Plain, Urban Area of Gotvand, South-West Iran. *Geopersia* **2013**, *3*, 35–46.
60. Dewana, B.R.; Prasetyo, S.Y.J.; Hartomo, K.D. Comparison of IDW and Kriging Interpolation Methods Using Geoelectric Data to Determine the Depth of the Aquifer in Semarang, Indonesia. *J. Ilm. Tek. Elektro Komput. Dan Inform.* **2022**, *8*, 215. [CrossRef]
61. Njeban, H.S. Comparison and Evaluation of GIS-Based Spatial Interpolation Methods for Estimation Groundwater Level in AL-Salman District—Southwest Iraq. *J. Geogr. Inf. Syst.* **2018**, *10*, 362–380. [CrossRef]
62. Arkoc, O. Modeling of Spatiotemporal Variations of Groundwater Levels Using Different Interpolation Methods with the Aid of GIS, Case Study from Ergene Basin, Turkey. *Model. Earth Syst. Environ.* **2022**, *8*, 967–976. [CrossRef]
63. Noori, S.; Ebrahimi, K.; Liaghat, A.-M.; Hoorfar, A.-H. Comparison of Different Geostatistical Methods to Estimate Groundwater Level at Different Climatic Periods. *Water Environ. J.* **2013**, *27*, 10–19. [CrossRef]
64. Hashemi Tameh, M.A.; Mazandarani Zadeh, H.; Arasteh Daneshkar, P. A Novel Solution to Define the Optimum Number and Location of New Wells to Improve Groundwater Level Map. *Procedia Eng.* **2016**, *154*, 252–259. [CrossRef]
65. Chang, L.-C.; Chu, H.-J.; Chen, Y.-W. A Fuzzy Inference System for the Conjunctive Use of Surface and Subsurface Water. *Adv. Fuzzy Syst.* **2013**, *2013*, 128393. [CrossRef]
66. Isazade, V.; Qasimi, A.B.; Toomanian, A.; Isazade, E. The Effect of Drought Phenomenon on the Surface of Groundwater Aquifer in Qazvin Plain in Iran. *J. Appl. Sci. Technol. Trends* **2023**, *4*, 80–85. [CrossRef]